

## **Nanofluid Predication Of Lid Driven Mixed Convection In Square Cavity With Adiabatic Elliptic Body**

**Hasan Shakir Majdi<sup>†</sup>, Azher M. Abed<sup>‡</sup>, Laith Jaafer Habeeb<sup>††</sup>**

<sup>†</sup>Chemical and Petroleum Industries Engineering Department / Al-Mustaqbal University College

<sup>‡</sup>Department of Air Conditioning and Refrigeration Techniques Engineering / Al-Mustaqbal University College

<sup>††</sup>Training and Workshop Center, University of Technology

E-mail: [Hasanshker1@gmail.com](mailto:Hasanshker1@gmail.com); [azhermuhson@mustaqbal-college.edu.iq](mailto:azhermuhson@mustaqbal-college.edu.iq); [20021@uotechnology.edu.iq](mailto:20021@uotechnology.edu.iq)

**ABSTRACT:** Numerical investigation of the mixed convection heat transfer of Al<sub>2</sub>O<sub>3</sub> water-nanofluid in a square cavity containing an adiabatic elliptic body. The top wall is moved as lid-driven and maintained at T<sub>h</sub>, while the bottom wall is cooled isothermally at T<sub>c</sub>. The stream function–vorticity scheme was used to solve the continuity, momentum, and energy equations. The results were validated by comparison the code results used in the present study with the previous results and found to be in very good agreement. The Richardson number was fixed at 1.0 (mixed convection). The temperature difference values between the hot and cold walls were  $\Delta T=1$  and 10. Different values of nanoparticles volume fraction were used ( $\phi =0, 0.02, 0.04, 0.08, 0.1, 0.15$ ). Two positions of elliptic body were used: horizontal and vertical. Results show that there is a slight effect for changing the position of inner body from horizontal to vertical position on the behavior of streamlines, thermal patterns, skin friction factor and average Nusselt number on the moving top wall. Moreover, the average heat transfer rate increases with increase in nanoparticles volume fraction and temperature gradient.

**KEYWORDS:** mixed convection, cavity, driven-lid, square, elliptic body

### **INTRODUCTION**

Lid-driven flows in enclosures are pertinent to different mechanical engineering applications such as electronic equipment cooling, solar collectors, oil extractions, and heat exchangers [1]. The forced convection is driven by moving any wall in the enclosure. While the natural convection is resulted from the temperature gradient between throughout the enclosure walls. Recently, many researchers studied the mixed convection in a cavity with different geometries and thermal boundary conditions.

Chen and Cheng [1] used a lid-driven arc-shape enclosure with different ranges of Grashof number and Reynolds number. Combined convection heat transfer from electronic equipment component with various positions of an enclosure was numerically investigated by Sattar and Khalid [2] using by primitive variables method. He proved that the heat transfer rate depends on the position of hot wall. M. Sharif [3] proved that the inclination angle of rectangular driven cavity played important role in the heat transfer enhancement. Chaves et al. [4] used porous media to enhance the heat transfer process in a semi porous open cavity. Porous Darcy–Brinkman medium in a rectangle lid-driven cavity was also used by Wang [5]. It was concluded that the presence of porous media led to decreasing the eddies effect. The active technique of heat transfer enhancement by vibration was used Chung and Vafai [6]. It was observed that the influences of vibration were significant only at high Darcy and Reynolds numbers. Irwan et. al. [7] studied the effect of porosity on the hydrodynamic boundary layer velocity in a square lid-driven cavity. Nemati et al. [8] used H<sub>2</sub>O-Cu, CuO or Al<sub>2</sub>O<sub>3</sub> nanofluids to improving the heat transfer by mixed convection in a lid-driven cavity. It was concluded that the increasing of moving wall velocity led to decreasing the effects of nanoparticles volume fraction. Rahman et al. [9] concluded that three convective regions were found in an inclined lid-driven triangular cavity filled with H<sub>2</sub>O-Cu nanofluid. Laith [10] found that the heat transfer rate increases with increase in porosity for the the case of moving wall. Aly and Ahmed [11] studied the mixed convective in a saturated cavity. The results showed that the mechanism of heat transfer and fluid field were strongly affected by the permeability ratio. Three flow regimes in an inclined triangular lid-driven cavity were observed by Chin-Lung and Yun-Chi [12]. The influences of the buoyancy forces were observed by Burgos et al. [13] to be neglected in open square cavity for Richardson

number less than 0.1. Zeghibid and Bessaïh [14] found the position of heat source in a lid-driven square cavity affected on the thermal patterns and flow fields. Kareem et al. [15] concluded that the aiding flow of SiO<sub>2</sub>-H<sub>2</sub>O in trapezoidal lid-driven cavity gave the highest heat transfer rates than other nanofluids. Kefayati and Tang [16] noticed that the heat transfer process in lid-driven cavity was enhanced significantly with increase in Hartmann number. Mohammed et a. [17] comprises a mathematical analysis of natural convection heat transfer in a horizontal elliptic cavity containing eccentric circular cylinder with different aspect ratios using Al<sub>2</sub>O<sub>3</sub>/water nanofluid. Results show that the angular distribution of local Nusselt number for the inner and outer cylinders depends on Rayleigh number, aspect ratio, nanoparticles volume fraction, and eccentric of inner cylinder. Lid driven was used in different shape cavities to study its influence on the heat transfer characteristics. It was found that Forced convection in lid-driven cavities is resulted from the lid movement which causes shear flow. While, natural convection is resulted of buoyancy driven associated with temperature gradient throughout the enclosure [18-20]. Dhahad et al. [21] studied the mixed convection heat transfer coefficient in a cavity using several ports configurations. The heat transfer have been studied in enclosed cavity with several shaped cavities and positions [22-25]. Inner cylinder was inserted in the cavity to increase the heat transfer [24]. Porous media was also fitted in the cavity to increase the heat transfer [25].

An investigation of the combined free-forced convection heat transfer in a square lid-driven cavity containing an adiabatic elliptic body are carried out numerically. The top wall is moved as lid-driven and maintained at T<sub>h</sub>, while the bottom wall is cooled isothermally at T<sub>c</sub>. The stream function–vorticity scheme was used to solve the continuity, momentum, and energy equations.

### MATHEMATICAL MODEL

#### Governing Equations

A steady two-dimensional, laminar flow and mixed convection heat transfer in a square lid-driven enclosure with inner elliptic body and filled with nanofluid is studied numerically. The based fluid is water with Al<sub>2</sub>O<sub>3</sub> nanoparticles. The vertical walls of the enclosure and the inner elliptic body are adiabatically insulated. While, the hot top wall is isothermally heated at temperature T<sub>h</sub> and the bottom wall is isothermally cooled at a temperature T<sub>c</sub> such that T<sub>h</sub> > T<sub>c</sub>. The top wall is moving at a constant velocity U. The physical domain studied in this work is shown in Fig. 1. The H<sub>2</sub>O-Al<sub>2</sub>O<sub>3</sub> nanofluid in the present work is considered as a single phase. Table 1 represents the values of thermophysical properties for the nanoparticles and the fluid phase at Temperature equals to 300 K. The governing mass, momentum, and energy equations can be given as follows:

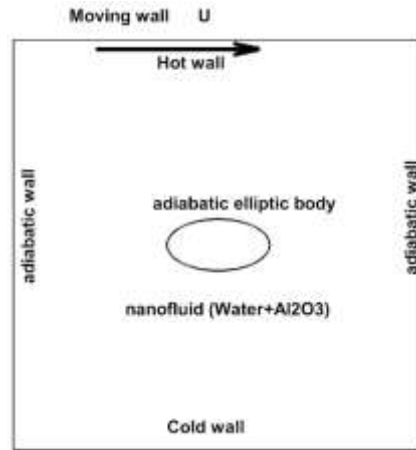


Figure 1. Physical domain

$$\frac{\partial U}{\partial X} + \frac{\partial V}{\partial Y} = 0, \quad (1)$$

$$U \frac{\partial U}{\partial X} + V \frac{\partial U}{\partial Y} = -\frac{\partial P}{\partial X} + \frac{1}{Re} \frac{\mu_{eff}}{\rho_{eff}} \left[ \frac{\partial^2 U}{\partial X^2} + \frac{\partial^2 U}{\partial Y^2} \right], \quad (2)$$

$$U \frac{\partial V}{\partial X} + V \frac{\partial V}{\partial Y} = -\frac{\partial P}{\partial Y} + \frac{1}{Re} \frac{\mu_{eff}}{\rho_{eff}} \left[ \frac{\partial^2 V}{\partial X^2} + \frac{\partial^2 V}{\partial Y^2} \right] + \frac{(\rho\beta)_{eff}}{\rho_{eff}} \frac{Gr}{Re^2} \theta, \quad (3)$$

$$U \frac{\partial \theta}{\partial X} + V \frac{\partial \theta}{\partial Y} = \frac{1}{Re Pr} \frac{\alpha_{eff}}{\alpha_{eff}} \left[ \frac{\partial^2 \theta}{\partial X^2} + \frac{\partial^2 \theta}{\partial Y^2} \right], \quad (4)$$

The above equations (1-4) are non-dimensionalized as given below:

$$U = \frac{u}{U_\infty}, \quad V = \frac{v}{U_\infty}, \quad X = \frac{x}{L}, \quad Y = \frac{y}{L}, \quad \theta = \frac{T - T_c}{T_h - T_c}, \quad P = \frac{p}{\rho_{eff} U_\infty^2}, \quad (5)$$

$$Re = \frac{U_\infty L}{\vartheta_f}, \quad Pr = \frac{\vartheta_f}{\alpha_f}, \quad Gr = \frac{g\beta L^3 (T_h - T_c)}{\vartheta^2}, \quad Ri = \frac{Gr}{Re^2}, \quad (6)$$

**Table 1.** Thermophysical properties of the base fluid and aluminum [26]

Physical properties	H <sub>2</sub> O	Al <sub>2</sub> O <sub>3</sub>
$C_p$ (J/kg.K)	4179	765
$k$ (W/m <sup>2</sup> .K)	0.613	25
$\mu$ (Pa.s)	0.000891	-
$\rho$ (kg/m <sup>3</sup> )	997.1	3970
$\beta$ (1/K)	0.00021	0.0000017

Boundary conditions

The dimensionless boundary conditions for the physical domain shown in Fig.1 are written as follows:

$$\begin{aligned} \frac{\partial \theta}{\partial Y} = 0, \quad U = V = 0, \quad X = 0 \\ \frac{\partial \theta}{\partial Y} = 0, \quad U = V = 0, \quad X = 1 \\ \theta = 0, \quad U = V = 0, \quad Y = 0, \\ \theta = 1, \quad U = 1, V = 0, \quad Y = 1. \end{aligned} \quad (7)$$

Thermophysical Properties of Nanofluid

The H<sub>2</sub>O-Al<sub>2</sub>O<sub>3</sub> nanofluid in the present work is considered as a single phase. Therefore; the base fluid and the nanoparticles are thermally balanced with each other. This leads to adopting the effective thermophysical properties. General correlations for the effective density, viscosity, thermal conductivity, thermal expansion coefficient, and specific heat of nanofluid have been developed and implemented in Fluent as given below; respectively [27].

$$\rho_{eff} = (1 - \varphi_p)\rho_f + \varphi_p\rho_s, \quad (8)$$

$$\mu_{eff} = (1.125 - 0.0007 \times T)\mu_f,$$

$$\varphi_p = 1\% \quad 20 \leq T[^\circ\text{C}] \leq 70, \quad (9)$$

$$\mu_{eff} = (2.1275 - 0.0215 \times T + 0.0002 \times T^2)\mu_f,$$

$$\varphi_p = 4\% \quad 20 \leq T[^\circ\text{C}] \leq 70, \quad (10)$$

$$\frac{k_{eff}}{k_f} = 1.0 + 1.0112\varphi_p + 2.437\varphi_p \left( \frac{47}{d_p(nm)} \right) - 0.0248\varphi_p \left( \frac{k_p}{0.613} \right), \quad (11)$$

$$\beta_{eff} = (-0.479\varphi_p + 9.3158 \times 10^{-3}T - \frac{4.7211}{T^2}) \times 10^{-3}$$

$$0 \leq \varphi_p \leq 0.04 \quad 10 \leq T[^\circ\text{C}] \leq 40, \quad (12)$$

$$c_{eff} = \frac{(1 - \varphi_p)\rho_f c_f + \varphi_p \rho_{sp} c_p}{\rho_{eff}}, \quad (13)$$

### Numerical Solution

Fluent 6.3 commercial program is used to solve the governing equations subject to considered boundary conditions. The grids are generated by using Gambit software. The grid independency is shown in Fig. 2. The number of grids used in the present study is 10,201. Time independent solver and laminar model are used for the present simulation. The pressure-velocity equations coupling is obtained using Simple scheme and solved sequentially. A second order upwind scheme is employed for the combined free-forced convection. The thermo-physical properties described above are obtained in the Fluent. When the residuals for continuity and momentum equations attain  $10^{-6}$ , the simulation is terminated. While, when the residual for energy equation attains  $10^{-8}$ , the simulation is terminated. The local Nusselt number based on the length of the square cavity is given as:

$$Nu_L = \frac{k_{eff}}{k_f} \frac{\partial \theta}{\partial Y} \Big|_{Y=1} \quad (14)$$

The average Nusselt number of the hot wall can be obtained by integrating the local Nusselt number along the wall as:

$$Nu_m = \int_0^1 Nu_L(X) dX \quad (15)$$

The local friction factor  $f_x$  on the moving lid related to the local shear stress  $\tau_x$  is calculated as follows:

$$f_x = \frac{\tau_x}{\rho u_o^2} = \frac{\mu}{\rho u_o^2} \frac{\partial u}{\partial y} \Big|_{moving\ lid} \quad (16)$$

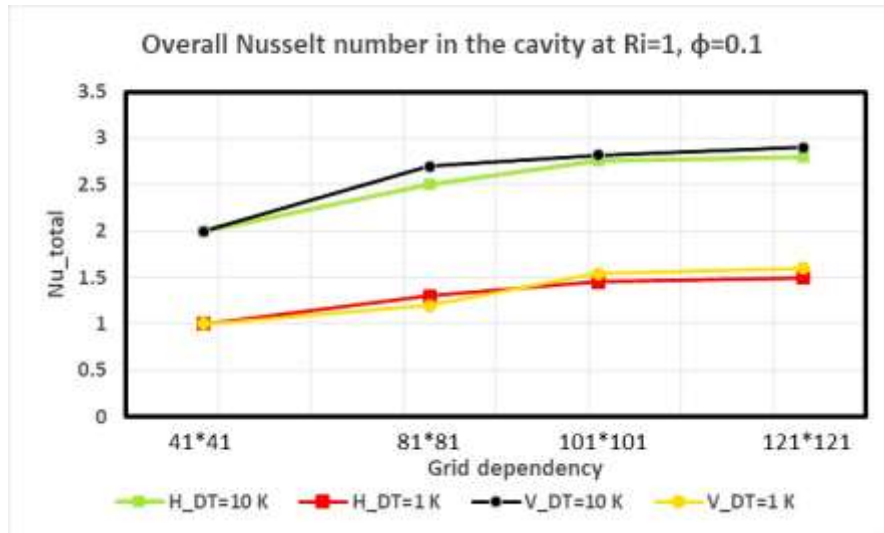


Figure 2. Grid independency

### Validation

To validate the present results, the numerical results extracted from the present code was compared with the numerical results worked by Iwatsu et al. [28] as shown in Fig. 3. This figure represents a case study of combined free-forced convection heat transfer in a lid-driven square cavity with inner circular body. In this figure, isotherms are on the left and streamlines are on the right) in the case of upward moving left wall, (a) adiabatic, (b) conductive ( $k=0.001$ ), and (c) isothermal ( $\theta = 0.5$ ) for

$Gr=10^6$ ,  $Pr=0.71$ ,  $Re=1000$ ,  $c=0.5$  and  $R=0.15$ . It can be seen that the two code results are identical with a very small difference as shown in Table 2.

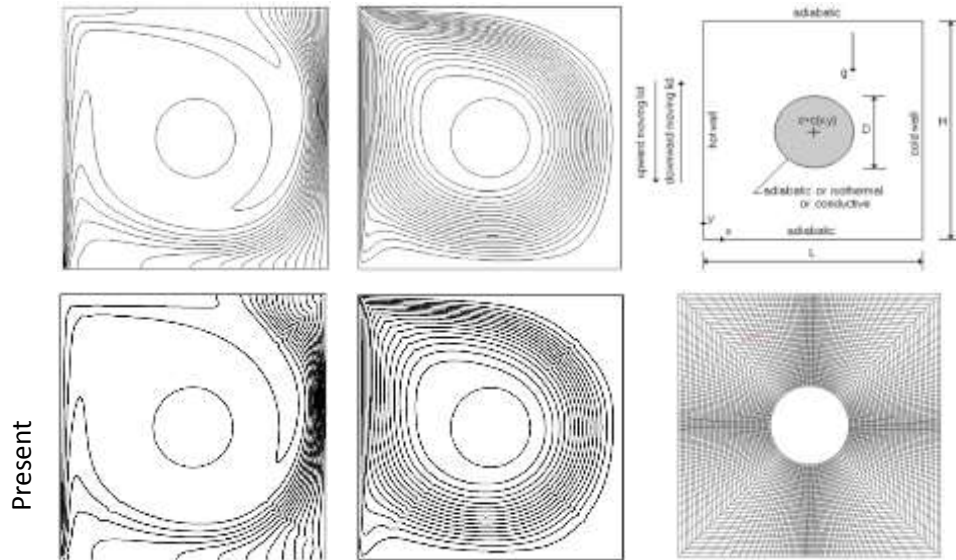


Figure 3. Code validation

Table 2. Average Nusselt numbers for the present work and the work of Iwatsu et al. [28].

Ri	Iwatsu, R	Present results	Error %
1.0	1.34	1.341	0.1
0.01	6.29	6.288	0.03

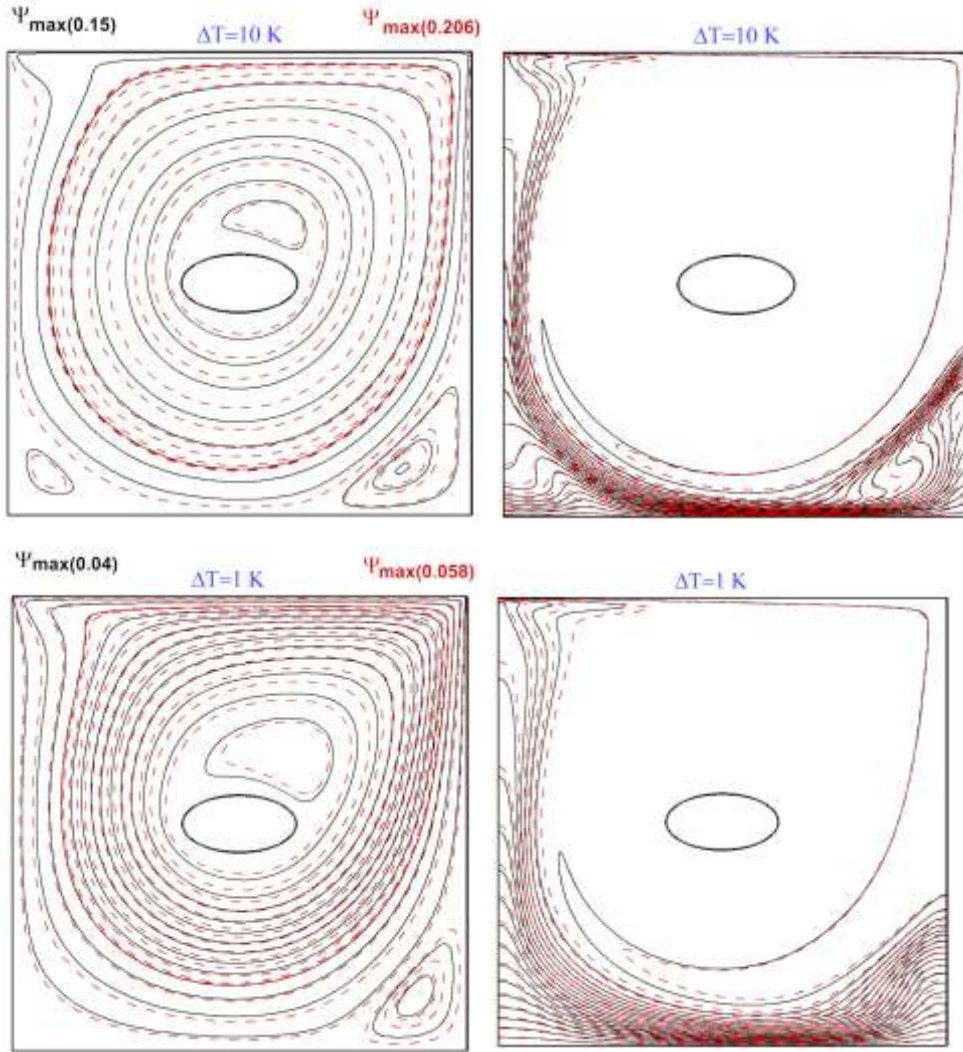
## RESULTS AND DISCUSSION

### Streamlines and isotherms

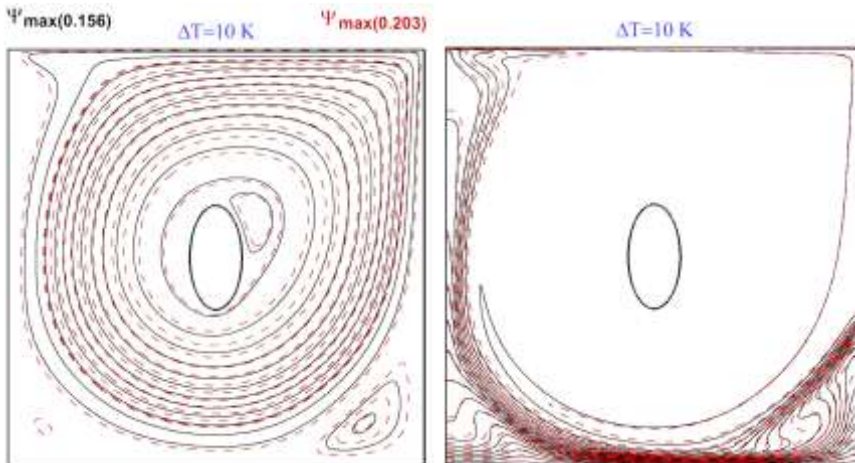
The effect of temperature gradient ( $\Delta T=1$  K and 10 K) on streamlines and isotherms inside lid-driven cavity filled with water only (solid black line  $\varphi = 0$ ) or  $H_2O-Al_2O_3$  nanofluid (dashed red line  $\varphi = 0.1$ ) and containing horizontal and vertical adiabatic elliptic body is shown in Fig.4 and Fig.5; respectively. The Richardson number is fixed at 1 (mixed convection)

It is shown that at low temperature gradients ( $\Delta T=1$  K), the shear force resulted from moving the top wall is dominant. In this case, the fluid motion is obtained by recirculating eddies near the top lid-driven. The isotherms are regulated close to the left and bottom walls causing a steep temperature gradient at these regions. At low temperature gradients, the vorticity seems to be weak (weak stream function,  $\psi = 0.04$ ). The stream function increases with using nanofluid ( $\psi = 0.058$ ). As temperature gradient increases to  $\Delta T=10$  K, the free convection currents grew and create circulation. This additional supporting to the main vorticity deviate towards the lower wall of cavity causing stronger flow field. The stream functions for the case of using the based fluid only or nanofluid are ( $\psi = 0.15$  and  $0.206$ ); respectively. It is shown from Fig.4 and Fig. 5 that, there is a slight effect for changing the position of inner body from horizontal to vertical position on the behavior of streamlines and thermal patterns. The stream functions for  $\Delta T=10$  K with and without nanoparticles are 0.156 and 0.203. While, these values decrease as  $\Delta T$  decreases to 1 K ( $\psi = 0.044$  and  $0.057$ ); respectively. The isotherms relatively change as the temperature gradient increases from  $\Delta T=1$  K to 10 K because of the thermal equilibrium between the buoyancy force and the inertia force. It is observed that in the region near to the hot top wall, the isotherms lines are thin, while the natural convection currents are more pronounced near at the lower and left regions of cavity because the higher temperature gradients at these regions.





**Figure 4.** Streamline (left) and temperature contour (right) for lid driven cavity with nanofluid with horizontal adiabatic elliptic body (solid black line  $\phi=0$ , and dashed red line  $\phi=0.1$ ).



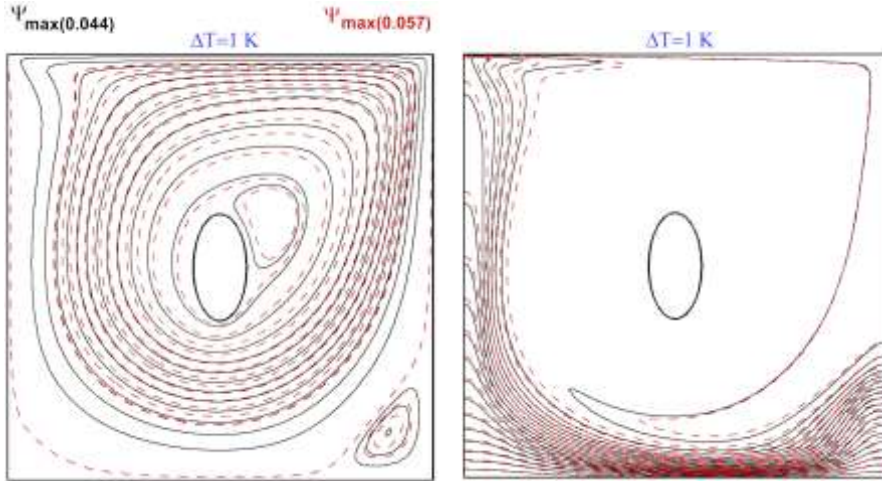


**Figure 5.** Streamline (left) and temperature contour (right) for lid driven cavity with nanofluid with vertical adiabatic elliptic body (solid black line  $\phi=0$ , and dashed red line  $\phi=0.1$ )

### Nusselt numbers

The local Nusselt number along the hot Top wall length for horizontal and vertical positions of inner elliptic body ( $\Delta T=1$  K and 10 K) at different nanoparticles volume fractions ( $\phi = 0, 0.08, 0.15$ ) are shown in Figures 6-9; respectively. It is noticed that the local Nusselt number increases at a small region near the left side wall for all values of nanoparticles volume fraction because the strong secondary and primary flows at this region. Then, it begins to decrease sharply until reaches a minimum value at the right end of top wall because of decreasing the thermal boundary layer. It is shown also that from these figures that the local Nusselt number increases with increase in nanoparticles volume fraction only at the first half of hot top wall. While, there is no effect for nanoparticles volume fraction on the local Nusselt number at the second half of moving top wall.

The variation of overall Nusselt number in the cavity and the average Nusselt number for the moving hot wall with changing the nanoparticles volume fraction for horizontal and vertical positions of inner elliptic body ( $\Delta T=1$  K and 10 K) are shown in Figures 10 and 11; respectively. It is shown that there is no effect for changing the position of inner elliptic body on the overall heat transfer rate in the cavity and the average heat transfer rate on the hot wall. This can be attributed to the small volume of this body which generates a small handicap to the fluid flow. Additionally, this inner body is far from the active regions of thermal and flow fields. Generally, it is noticed that the overall and average heat transfer rate increase with increase in nanoparticles volume fraction and temperature gradient.

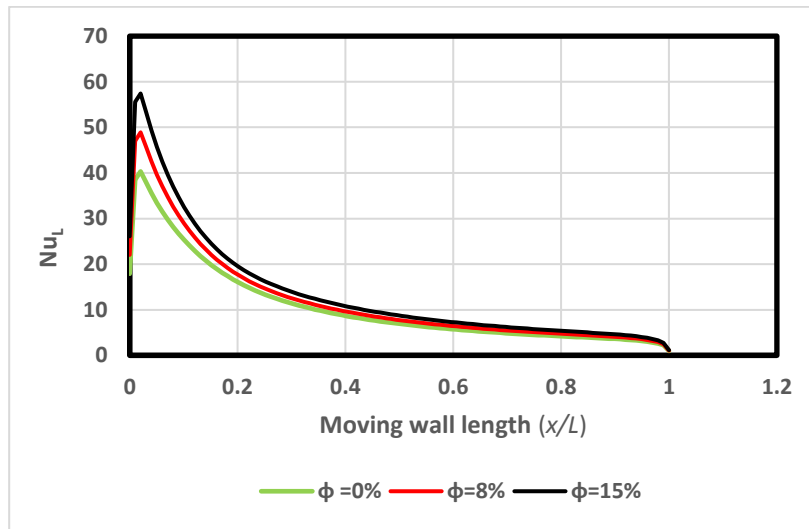


**Figure 6.** Local Nusselt number along the moving wall for horizontal inner body, ( $\Delta T=10$  K).

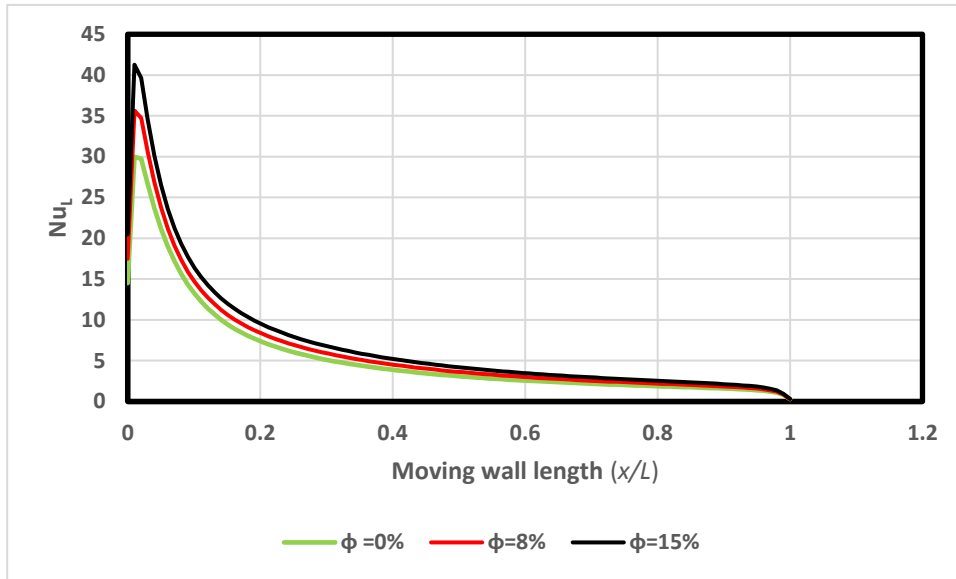


**Figure 7.** Local Nusselt number along the moving wall for horizontal inner body, ( $\Delta T=1$  K).

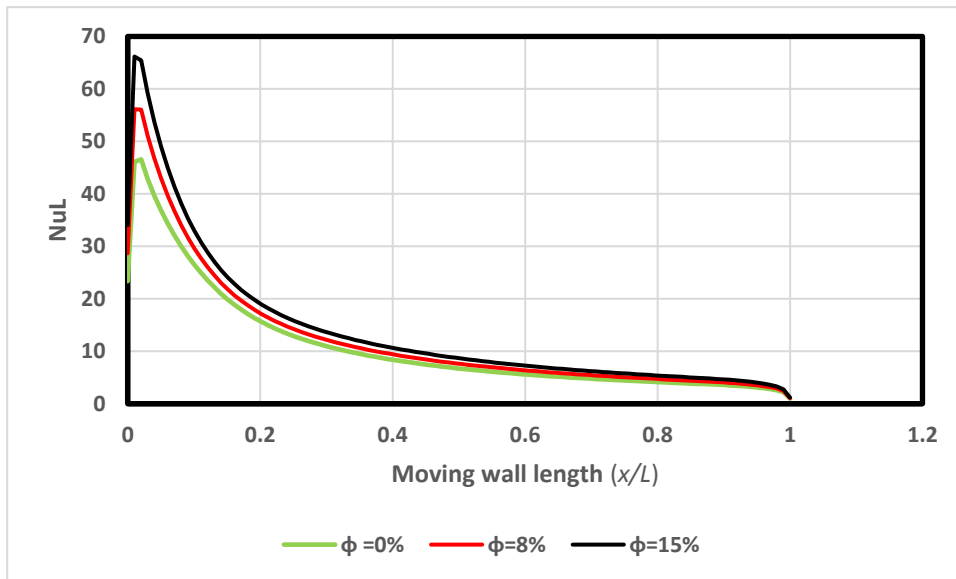


**Figure 8.** Local Nusselt number along the moving wall for vertical inner body, ( $\Delta T=10$  K).



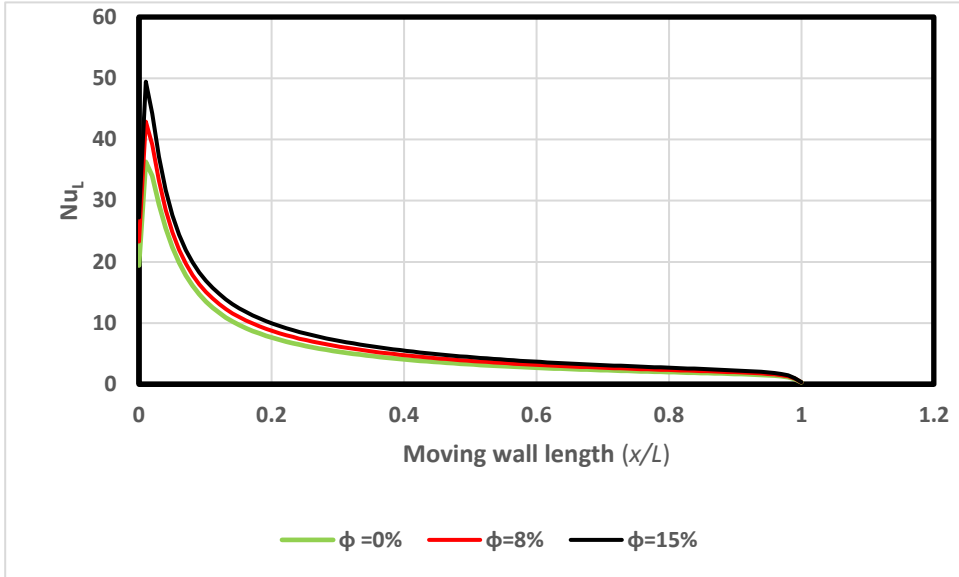


Figure 9. Local Nusselt number along the moving wall for vertical inner body, ( $\Delta T=1$  K).

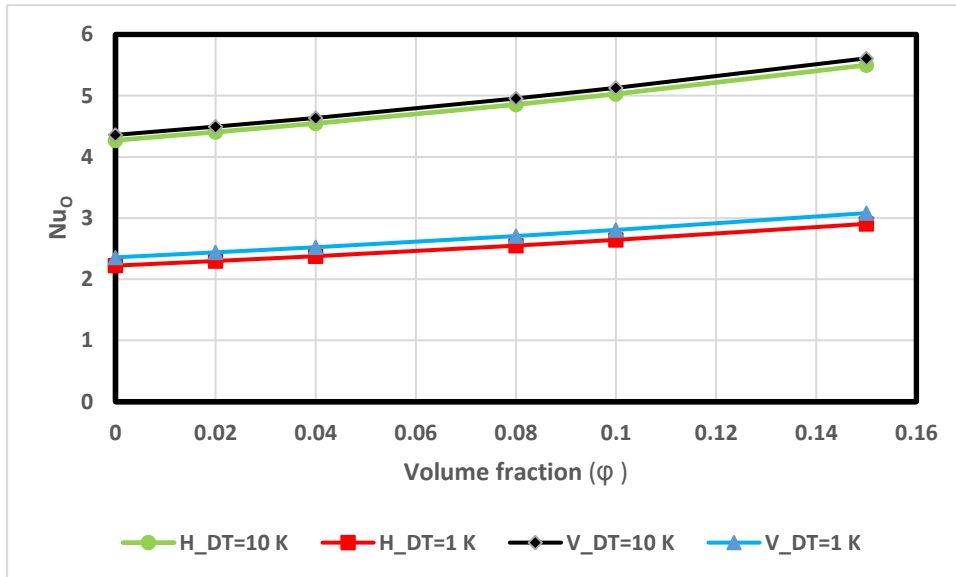
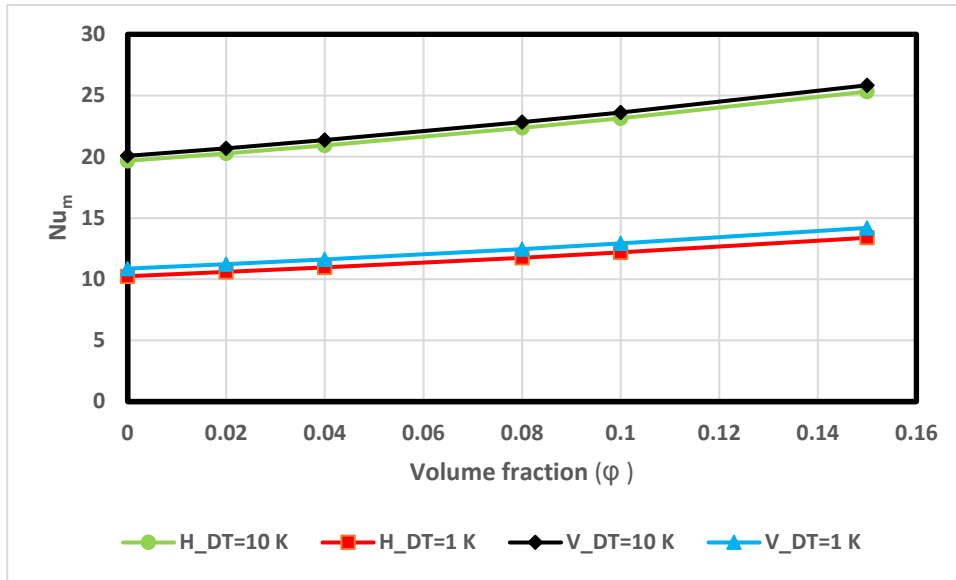


Figure 10. Overall Nusselt number in the cavity versus nanoparticles volume fraction.



**Figure 11.** Average Nusselt number on moving wall in the cavity versus nanoparticles volume fraction

Skin friction factor

The variation of average skin friction factor over moving wall in the cavity with changing the nanoparticles volume fraction for horizontal and vertical positions of inner elliptic body ( $\Delta T=1$  K and 10 K) is shown in Fig. 12. It is noticed that there is no effect for changing the position of inner elliptic body on the skin friction factor on the hot moving wall. Moreover, the skin friction factor increases with increase in nanoparticles volume fraction due to increasing the thermal conductivity of the based fluid by adding nanoparticles. Additionally, the skin friction factor increases with increase in temperature gradient in the cavity because of increasing the shear force on the moving hot wall.

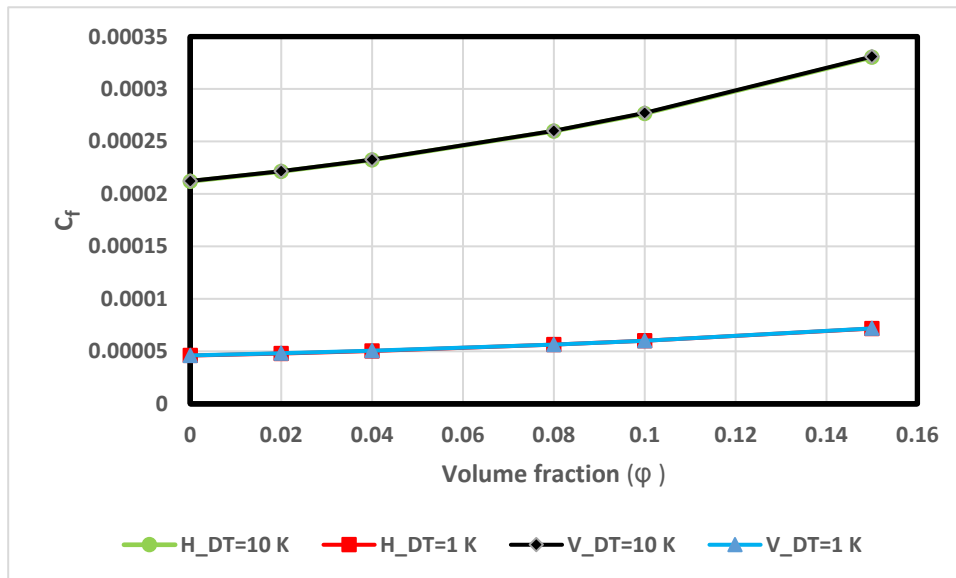


**Figure 12.** Average skin friction factor over moving wall in the cavity versus nanoparticles volume fraction

CONCLUSIONS

1. There is a slight effect for changing the position of inner body from horizontal to vertical position on the behavior of streamlines, thermal patterns, skin friction factor and average Nusselt number on the moving top wall.
2. The local Nusselt number increases at a small region near the left side wall for all values of nanoparticles volume fraction.
3. There is no effect for nanoparticles volume fraction on the local Nusselt number at the second half of moving hot top wall.
4. The average heat transfer rate for the moving hot wall and the overall Nusselt number in the cavity increase with increase in nanoparticles volume fraction and temperature gradient.
5. The skin friction factor increases with increase in nanoparticles volume fraction and temperature gradient in the cavity.

### Nomenclature

$f_x$	local friction factor	$u, v$	velocity components in x- and y-directions, respectively
$g$	gravitational acceleration	$U, V$	dimensionless velocity components in x- and y-directions, respectively
$L$	reference length	$u_o$	constant velocity of moving lid
$Gr$	Grashof number	$U_\infty$	<b>reference velocity</b>
$h$	overall heat transfer coefficient	$x, y$	rectangular coordinates
$h_x$	local heat transfer coefficient	$X, Y$	dimensionless rectangular coordinates
$J$	Jacobian of coordinate transformation	$\alpha$	fluid thermal diffusivity
$\kappa$	thermal conductivity of fluid	$\beta$	coefficient of volume expansion for fluid
$N$	number of corrugations	$\lambda$	amplitude
$Nu_L$	Local Nusselt number	$\varphi$	Solid volume fraction
$Nu_m$	meanl Nusselt number	$\mu$	dynamic viscosity of fluid
$Pr$	Prandtl number	$\vartheta$	kinematic viscosity of fluid
$Re$	Reynolds number	$\tau_x$	local shear stress
$Ri$	Richardson number ( $Ri = Gr/Re^2$ )	Subscript	
$T$	fluid temperature	f	fluid
$T$	dimensionless temperature	p	nanoparticles
$T_h$	higher temperature at side walls	eff	effective
$T_l$	lower temperature at base wal		

### REFERENCES

- [1] C.L. Chen, Chin-Hsiang Cheng, “Experimental and numerical study of mixed convection and flow pattern in a lid-driven arc-shape cavity”, *Heat Mass Transfer* (2004) 41: 58–66.
- [2] S.J. Habeeb, Khalid A. Ismael, Jalal M. Jalil, “Mixed convection from electronic equipment component at different position an enclosure by primitive variables method”,
- [3] M. A. R. Sharif, “Laminar mixed convection in shallow inclined driven cavities with hot moving lid on top and cooled from bottom”, *Applied Thermal Engineering* 27 (2007) pp. 1036–1042.
- [4] C. A. Chaves, J. R. Camargo, and V. A. Correa, “Combined forced and free convection heat transfer in a semiporous open cavity,” *Sci. Res. Essay*, vol. Vol.3 (8), no. June 2014, pp. 333–337, 2008.
- [5] C.Y. Wang, “The recirculating flow due to a moving lid on a cavity containing a Darcy–Brinkman medium”, *Applied Mathematical Modeling* 33 (2009) 2054–2061.
- [6] Stephen Chung, Kambiz Vafai, “Vibration induced mixed convection in an open-ended obstructed cavity ”*International Journal of Heat and Mass Transfer* 53 (2010) 2703–2714.
- [7] M.A. Mohd Irwan, A. M. Fudhail, C.S. Nor Azwadi and G. Masoud, “Numerical Investigation of Incompressible Fluid Flow through Porous Media in a Lid-Driven Square Cavity”, *American Journal of Applied Sciences* 7 (10): 1341-1344, 2010.

- [8] H. Nemati, M. Farhadi, K. Sedighi, E. Fattahi, A. A. R. Darzi, "Lattice Boltzmann simulation of nanofluid in lid-driven cavity", *International Communications in Heat and Mass Transfer* 37 (2010) 1528–1534.
- [9] M. M. Rahman, M. M. Billah, A. T. M. M. Rahman, M. A. Kalam, A. Ahsan, "Numerical investigation of heat transfer enhancement of nanofluids in an inclined lid-driven triangular enclosure", *International Communications in Heat and Mass Transfer*, Volume 38, Issue 10, December 2011, Pages 1360-1367.
- [10] L. J. Habeeb, "Free Convective Heat Transfer in an Enclosure Filled with Porous Media with and without Insulated Moving Wall", *World Academy of Science, Engineering and Technology* 69, 2012.
- [11] A.M. Aly and Sameh E. Ahmed, "An incompressible smoothed particle hydrodynamics method for natural/mixed convection in a non-Darcy anisotropic porous medium", *International Journal of Heat and Mass Transfer*, Volume 77, October 2014, pp. 1155-1168.
- [12] C.L. Chen and Yun-Chi Chung, "NUMERICAL STUDY ON MIXED CONVECTION HEAT TRANSFER IN INCLINED TRIANGULAR CAVITIES", *Numerical Heat Transfer, Part A*, 67: 651–672, 2015.
- [13] J. Burgos, I. Cuesta, C. Salueñ, "Numerical study of laminar mixed convection in a square open cavity", *International Journal of Heat and Mass Transfer* 99 (2016) 599–612.
- [14] I. Zeghibid and Rachid Bessaïh, "Mixed Convection in a Lid-Driven Square Cavity With Heat Sources Using Nanofluids", *FDMP*, vol.13, no.4, pp.251-273, 2017
- [15] A. K. Kareem, H. A. Mohammed, Ahmed Kadhim Hussein, Shian Gao, "Mixed convection heat transfer in a lid-driven trapezoidal enclosure filled with nanofluids", *International Communications in Heat and Mass Transfer*, August 2016, DOI: [10.1016/j.icheatmasstransfer.2016.08.010](https://doi.org/10.1016/j.icheatmasstransfer.2016.08.010)
- [16] GH.R. Kefayati, H. Tang, "MHD mixed convection of viscoplastic fluids in different aspect ratios of a lid-driven cavity using LBM", *International Journal of Heat and Mass Transfer* 124 (2018) 344–367.
- [17] A.A. Mohammed, Sanaa Turki Mousa Al- Musawi, Sadoon K. Ayed, Aseel Alkhatat, Laith Jaafer Habeeb, "Natural Convection Heat Transfer in Horizontal Elliptic Cavity with Eccentric Circular Inner Cylinder", *Journal of Mechanical Engineering Research and Developments*, Vol. 43, Special Issue: Mechanics and Energy, pp. 340-355, 2020.
- [18] M. M. Al-azzawi, Ayad K. Hassan, Humam Kareem Jalghaf, Laith Jaafer Habeeb, "Numerical Study of Lid Driven Mixed Convection in Inclined Wavy Cavity", *Journal of Mechanical Engineering Research and Developments*, Vol. 43, No. 6, pp. 184-196, 2020.
- [19] M. A. S. Mustafa, Hasanen Mohammed Hussain, Auday Awad Abtan, Laith Jaafer Habeeb, "Review on Mixed Convective Heat Transfer in Different Geometries of Cavity with Lid Driven", *Journal of Mechanical Engineering Research and Developments*, Vol. 43, Special Issue: Mechanics and Energy, pp. 12-25, 2020.
- [20] A. N. A. Saieed, Mustafa Abdul Salam Mustafa, Sadoon K. Ayed, Laith Jaafer Habeeb, "Review on Heat Transfer Enhancement in Cavity with Lid Driven", *Journal of Mechanical Engineering Research and Developments*, Vol. 43, Special Issue: Mechanics and Energy, pp. 356-373, 2020.
- [21] H.A. Dhahad, Gazy F. Al-Sumaily, Laith J. Habeeb, Mark C. Thompson, "The Cooling Performance of Mixed Convection in a Ventilated Enclosure with Different Ports Configurations", *Journal of Heat Transfer, ASME*, DECEMBER 2020, Vol. 142 / 122601-1-18, pp. 62-74, 2020.
- [22] R.C. Al-Zuhairy, Muna Hameed Alturaihi, Faez Abid Muslim Abd Ali, Laith Jaafer Habeeb, "Numerical Investigation of Heat Transfer in Enclosed Square Cavity", *Journal of Mechanical Engineering Research and Developments*, Vol. 43, No. 6, pp. 388-403, 2020.
- [23] H. J. Jaber, Ali Abd Al-Nabi Abaas, Faez Abid Muslim Abd Ali, Laith Jaafer Habeeb, "Cooling of a Vertically Oriented Air-Ventilated Square Cavity", *Journal of Mechanical Engineering Research and Developments*, Vol. 43, No. 6, pp. 23-38, 2020.

- [24] A.A. Mohammed, Sanaa Turki Mousa Al- Musawi, Sadoon K. Ayed, Aseel Alkhatat, Laith Jaafer Habeeb, "Natural Convection Heat Transfer in Horizontal Elliptic Cavity with Eccentric Circular Inner Cylinder", *Journal of Mechanical Engineering Research and Developments*, Vol. 43, Special Issue: Mechanics and Energy, pp. 340-355, 2020.
- [25] M. A. Mashkour, Laith Habeeb, Hazim Jassim Jaber, "Heat Transfer in a partially Opened Cavity Filled with Porous Media", 3rd Scientific International Conference 2013 / Najaf, pp. 601-614.
- [26] M.A. Mansour, Ahmed, S.E. (2013). Mixed convection in double lid-driven enclosures filled with Al<sub>2</sub>O<sub>3</sub>-water nanofluid. *Journal of Thermophysics and Heat Transfer*, vol. 27, no. 4, p. 707-718, DOI:10.2514/1.T4102.
- [27] Y. Taamneh, Kahled Bataineh, "Mixed Convection Heat Transfer in a Square Lid-Driven Cavity Filled with Al<sub>2</sub>O<sub>3</sub>-Water Nanofluid", *Strojniški vestnik - Journal of Mechanical Engineering* 63(2017)6, 383-393.
- [28] R. Iwatsu, Hyun, J.M., Kuwahara, K., 1993. Mixed convection in a driven cavity with a stable vertical temperature gradient. *Int. J. Heat Mass Transfer* 36, 1601–1608.